Bioengineering Research

A Promising Stimuli-Responsive Nanocomposite as a Theranostic Agent for Targeted Delivery

Navid Rabiee [1,2], **Mohammad Rabiee** [3]

[1]Division of Chemistry, Advanced Technologies Research Group, Tehran, Iran
[2]Division of Diseases, Advanced Technologies Research Group, Tehran, Iran
[3]Biomaterial Group, Department of Biomedical Engineering, Amirkabir University of Technology, Tehran, Iran
Correspondence to: Rabiee M. (E-mail: mrabiee@aut.ac.ir)

Abstract

Introduction: A range of strategies for eliminate the cancer tissue have been used, consisting of medical operation, chemo and radiotherapy.

Objective: There is a significant issue about chemotherapy, the medications targeted delivery to object tissue cells is found challengeable because of the presence of numerous physical obstructions.

Materials and Methods: In the present study, we synthesized and characterized a novel and promising specific pH-stimuli-responsive tumor-targeted DDS. The synthesized magnetic nanoparticles (Nanocomposite) were fully characterized by FESEM, TEM, DLS, XRD and VSM.

Results: The morphology of Nanocomposite are acquired in semi-spherical shape with the specified diameters. The Capsaicin was successfully loaded Nanocomposite represented promising and admissible biocompatibility as well as showing higher toxicity versus SK-N-MC cells in comparison with control group.

Conclusion: Furthermore, uptake investigation proved that the effectively internalized Drug Delivery System (DDS). In addition, the in vitro assay represented that the synthesized Nanocomposite can act nearly fully pH stimuli-responsive and release the Capsaicin at controlled condition. MTT assay verified the higher toxicity of Capsaicin loaded into the Nanocomposite in comparison with the control group. MRI in vitro investigation demonstrated that the prepared Nanocomposite can utilized as MRI imaging agent.

Keyword: Capsaicin, nanocomposite, Cobalt Ferrite, Biocompatibility, ZSM-5

Received: 14 February 2019, Accepted: 9 March 2019

DOI: 10.22034/jbr.2019.84394

1. Introduction

In recent times, cancer actually turns into critical issues of Healthcare, as well as, medication procedure burden tremendous financial costs on people and authorities. By the record from Reliable References, in 2012, more than 8 million people with cancer passed away. It is normally anticipated which unfortunately trends of the number of cancer patients would definitely enhance to over 20 million by 2030 [1-7].

A range of strategies for eliminating the cancer tissue has been used, consisting of medical operation, chemo- and radiotherapy. There is a significant issue about chemotherapy; the medications targeted delivery to object tissue cells is found challengeable

because of the presence of numerous physical obstructions [8-15].

Nanotechnology is a new field of science that takes advantage of the peculiar properties of matter at the nanoscale. The extremely high ratio of surface area to mass that is typical of nanoparticles, allows them to interact efficiently with their environment, but yet they can act as contained carriers for their constituent molecules as opposed to the same molecules in solution. Nanoparticles are therefore promising carriers for targeted delivery of therapeutic agents. The particle size (ranging from a few nanometers to the micron range) can directly influence cell uptake. Although there is no consensus on the optimum size, many studies suggest that a size which is less than 100 nm provides stability in body fluids, a higher ability to penetrate biological membranes, and a better capacity to accumulate inside cells. Different nanocarriers such as liposomes, micelles, polymeric nanomaterials, mesoporous silica, gold, and magnetic nanoparticles have improved biomedical applications including drug and gene delivery. On the other hand, suitable functionalization of the nanoparticle surface, not only can increase specific targeting by ligand-recognition or enzyme-responsiveness but can also enable the monitoring of drug delivery by attached imaging reporters. Moreover, nanoparticle drug delivery vehicles significantly decrease the side-effects of drugs, (particularly anticancer chemotherapy) by increasing their water solubility and therefore decreasing the required overall dose [6, 14, 16-22].

Several types of magnetic nanoparticles (Nanocomposite) can be found broadly used as nanocarriers as well as, targeted contrast agents. Different stimuli-responsive-based modifications on the surface of these Nanocomposites could enhance the biocompatibility of these nanosystems whereas led to decrease in the off-target result. Cobalt-based nanosystems have significant magnetic and catalytic features that have been utilized widely in different biomedical applications [23-28].

Between several chemotherapeutic agents utilized with regards to cancer therapy, Capsaicin, trans-8-methyl-N-vanillyl-6-nonenamide, a natural compound that has been presented in red pepper demonstrated anti-carcinogenic, anti-mutagenic, and chemo-preventive in a large number of cancer, has gained significant attention due to the exclusive features. The scientists published several articles related to anti-carcinogenic, anti-mutagenic and chemo-preventive effect of Capsaicin by inducing apoptosis as well as anti-angiogenic and anti-metastatic activities [29-33].

In the present study, a novel $CoFe_2O_4$@ZSM-5 nanocomposite with freshly promising synthesis route, Egg-white (EW) which led to taking biocompatible nanocomposite has been revealed for controlled Capsaicin delivery along with monitoring by MRI study.

2. Materials and Methods

2.1. Materials

Dimethyl sulphoxide (DMSO), Cobalt (III) nitrate hexahydrate ($Co(NO_3)_2.6H_2O$), iron nitrate ($Fe(NO_3)_2.9H_2O$), Glutathione, Oleic Acid, sodium hydroxide, Capsaicin, ammonia solution ($NH_3{\cdot}H_2O$, 28% of ammonia), absolute ethanol (EtOH) and *N*-hydroxy succinimide (NHS) were purchased from Sigma-Aldrich (Germany). SK-N-MC neuroblastoma cell line (as model cancerous cell line) was obtained from Pastor Institute Cell bank (Tehran, Iran).

2.2. Characterizations

For the nanocomposite characterizations, Transmission electron microscopy (TEM, LEO 912AB electron microscope), Field emission scanning electron microscope (FESEM, MIRA3 TESCAN microscope), X-ray diffractometer (XRD), Vibrating sample magnetometer (VSM, Squid-VSM, Quantum Design, Germany) and Dynamic light scattering (DLS, Malvern Zeta Sizer ZS90, UK) was applied. For TEM, a fraction of the synthesized nanocomposite was fixed to the carbon film with a copper grid and dried. Morphology of the synthesized nanocomposite was investigated by applying SEM microscopy by dropping the diluted nanocomposite solution on glass slides and dried at room temperature. Hydrodynamic size of the nanocomposite was investigated by DLS evaluation. The structural investigation was investigated by X-ray diffraction, XRD patterns acquired with Cu Kα

radiation at 40 keV and 30 mA, and scanning rate was set to 2°min^{-1} in the 2θ range from 10° to 80°. Ultraviolet-visible spectra of the nanocomposite were assessed by UV-Vis Jasco-530 spectrophotometer. The hysteresis loop of the nanocomposite was measured at room temperature through the VSM with a maximum magnetic field of 10 and accelerating voltage of 15 kV.

2.3. Synthesis of $CoFe_2O_4$

Briefly, in the EW synthesis route, egg white was mixed with deionized water in 2:3 ratios. Afterward, the mixture had been strongly stirring at room temperature until a homogeneous solution was achieved. Then, a stoichiometry amount of Cobalt (III) and Iron (III) nitrate were separately dissolved in distilled water and poured into the first homogenous solution and stirred vigorously for 3 hours. In the next step, 25 mL of sodium hydroxide 3M was added and the final solution stirred up to pH = 12. Then, 1 mL Oleic acid as a chelating agent was added to the above suspension. The temperature of the suspension was raised to 80 ^oC with continued stirring for 2 hours. The product was cooled to room temperature, and the precipitate was separated by centrifuge, washed twice with distilled water and ethanol. The precipitate was dried at 65 ^oC (dark brown powder), calcined at 400 ^oC for 8 hours followed by recalcination at 800 ^oC for 4 hours and black powder was obtained.

2.4. Preparation of the $CoFe_2O_4$@ZSM-5 nanocomposite

Briefly, we have three beakers, in the first beaker 0.5 g $NaAl_2O_3$ was dissolved in 45 ml H_2O, in the second beaker 7.9 g Silicic acid was dissolved in 35 ml H_2O and in the third beaker 0.17 g the $CoFe_2O_4$ NPs were dispersed in 10 ml H_2O. After that, the solution of the first beaker added to the third beaker and vigorously stirred for 20min, following by that, the second beaker added to the mentioned solution under stirring vigorously. Eventually, the final mixture (suspension) inserted to a stainless Teflon and autoclaved at 200 ^oC for 48 hours. The final product was filtered twice, washed for triple times with ultra-pure water and dried at 65 ^oC.

2.5. Loading of capsaicin on $CoFe_2O_4$@ZSM-5 nanocomposite

Loading procedure of Capsaicin into the nanocomposite proceeded by injecting 300 µL of 15 mg Capsaicin in acetone to 5 mL dispersion of the 10 mg of $CoFe_2O_4$@ZSM-5. The mixture was then stirred at 600 rpm for 24 h. The product was separated from free Capsaicin by magnetic separation and several times washing with deionized water. Afterward, the purified Capsaicin loaded $CoFe_2O_4$@ZSM-5 were freeze dried. Loading efficiency of Capsaicin was measured using UV-Vis spectrophotometer at 280 nm.

2.6. *In* vitro drug release

To evaluate the drug release of Capsaicin loaded $CoFe_2O_4$@ZSM-5, 4 mg of the $CoFe_2O_4$@ZSM-5 was poured into a 10 mL tube containing 6 mL phosphate buffer saline (PBS) of pH=5.5 and pH=7.4 and 0.1% (w/v) Tween-80. The solutions were shaken at 37 °C at 200 rpm in an orbital shaker. The samples were centrifuged at 12,000 rpm for 15 minutes, and the supernatants were collected and stored at 4 °C. All samples were replaced by equivalent volumes of fresh medium. The obtained supernatants were measured for absorbance at 280 nm using a UV-Vis spectrometer. An identical standard of Capsaicin (0–10 µg/mL) was prepared, and absorbance was measured at 280 nm using the UV-Vis spectrometer to determine the amount of Capsaicin released from $CoFe_2O_4$@ZSM-5.

2.7. *In* vitro cytotoxicity

MTT (3-[4,5-dimethyl-thiazol-2-yl]-2,5-diphenyltetrazoliumbromide) cell proliferation assay was employed to assess *in vitro* cytotoxicity of Capsaicin and Capsaicin loaded $CoFe_2O_4$@ZSM-5. For this assay, SK-N-MC cell line, at an initial density of 2×10^3 cells per well, were seeded into 96-well plates in a volume of 200 µL DMEM (Dulbecco's Modified Eagle's Medium-High Glucose) and incubated overnight (100 IU/mL penicillin and 100 µg/mL streptomycin sulfate). Then, the medium was replaced with a fresh medium, containing PBS (as a control agent), Capsaicin and Capsaicin loaded $CoFe_2O_4$@ZSM-5 and followed by incubation for 48

hours at 37 ºC. Afterward, 10 µL of the MTT labeling reagent was transferred into each well. After incubation (4 hours), 100 µL DMSO was added to each well to dissolve the insoluble formazan crystals. Finally, after incubation (overnight at 37 ºC), the color intensity of solubilized formazan was assessed at 570 nm wavelength using a microplate reader (BioMate 3 UV-Vis spectrophotometer).

2.8. *In vitro* magnetic mesonance imaging

In order to evaluate *in vitro* MRI properties, synthesized $CoFe_2O_4$@ZSM-5 were dispersed in 3% (w/v) agarose solution. Formulations were placed into the MRI scanner and followed by running a number of spin-echo sequences to determine T_2 relaxation time. MRI solutions were scanned under a 3-Tesla clinical MRI scanner (Imam Khomeini Hospital, Tehran) at room temperature. The increase of relaxation rate (S^{-1}, $1/T_2$) with increasing the metal concentration was analyzed through linear regression analysis. The concentration of iron oxide used in each formula was modulated to be within 1.0-50 mg Fe/mL. MRI parameters involved to acquire images of each sample, were as below: echo time (TE= 15-120 ms), repetition time (TR= 1000 ms), number of echoes (NE= 8), number of excitations (NEX= 4), matrix size of 128 × 128, and field of view (15 mm × 15 mm). To measure of signal intensity, a manually drawn region of interest was used for each sample by DICOM Viewer software. Furthermore, relaxation rates ($r_2=1/T_2$) were extracted with mono exponential curve fitting the signal intensities versus echo time at different concentrations for each of the samples. For further analysis, T_2 relaxivities and r_2 ($mM^{-1}\ S^{-1}$) were calculated from the slope of T_2 values (relaxation rate) *vs* the metal concentration according to the equation:

$$r2= (A + C) \times \exp^{(-r2\times TE)}$$

2.9. Cellular uptake of $CoFe_2O_4$@ZSM-5 nanocomposite

The internalization of Capsaicin loaded $CoFe_2O_4$@ZSM-5 by SK-N-MC cells was analyzed through flow cytometry method. 4×10^5 cells were plated in 6-well dishes in 2 mL medium (DMEM) under standard culture conditions and incubated for 24 h. Afterward, media was replaced with 2 mL of serum-free medium containing Capsaicin or Capsaicin loaded $CoFe_2O_4$@ZSM-5 (40-100 µg/mL). After 12 hours of cell treatment, the cells were washed three times with cold PBS (pH= 7.4). Finally, the fluorescence intensity of Capsaicin per cell was quantified using a flow cytometer (FACScan, LYSIS II, Becton Dickinson) at the excitation wavelength of 280 nm and an emission wavelength of 316 nm.

3. Results and Discussion

3.1. Characterization of the nanocomposite

Surface morphology, size, and shape of the nanocomposite were investigated by FESEM, TEM and DLS analysis. The FESEM images approved the spherical morphology of the prepared Nanocomposite with negligible aggregation. Same as the FESEM images, The TEM images approved the formation of the Nanocomposite and spherical morphology of them (Figures 1 A-C).

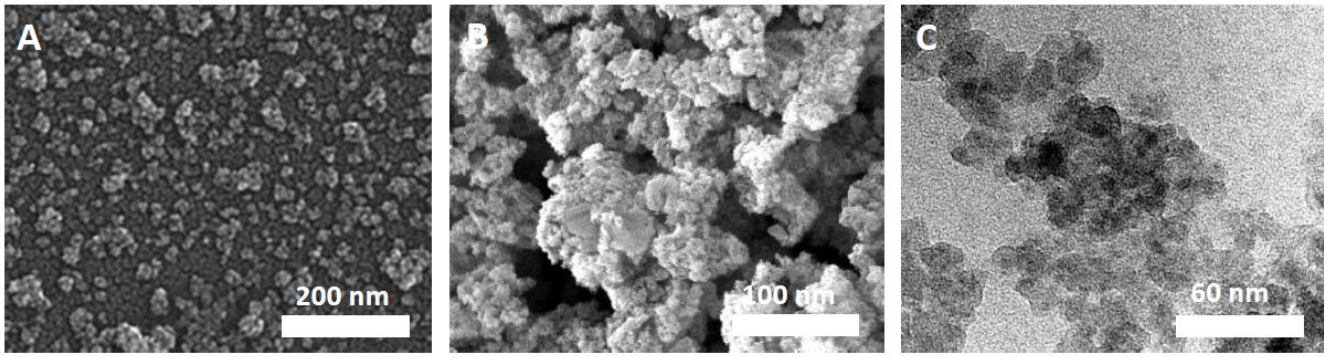

Figure 1. SEM images of the (A) $CoFe_2O_4$ and (B) $CoFe_2O_4$@ZSM-5 nanocomposite. (C) TEM image of the $CoFe_2O_4$@ZSM-5 nanocomposite.

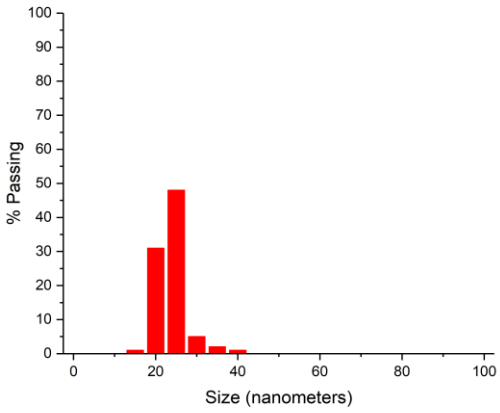

Figure 2. DLS of the $CoFe_2O_4$@ZSM-5 nanocomposite

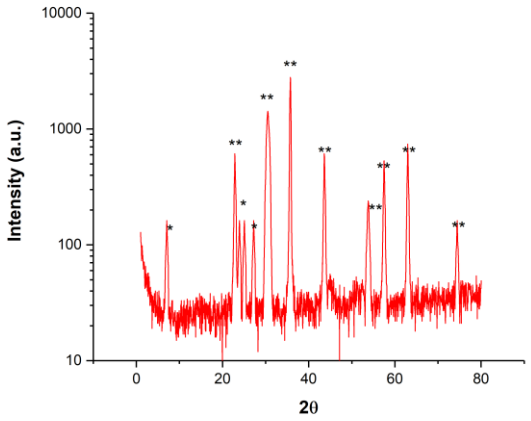

Figure 3. XRD pattern of the $CoFe_2O_4$@ZSM-5 nanocomposite.

In addition, the DLS was applied to determine the average diameter of $CoFe_2O_4$@ZSM-5 Nanocomposite, which the data's were specified average diameter of $CoFe_2O_4$@ZSM-5 Nanocomposite about 24 nm (Figures 2). Furthermore, increasing in the average size of the Nanocomposite modified by ZSM-5 had been predicted.

Evaluation the surface charge of the Nanocomposite had been proceeded by surface zeta potential. Zeta potential of $CoFe_2O_4$@ZSM-5 Nanocomposite were acquire 19.2 mV. It has been proved that loading of the Capsaicin led to neutralization of the remained positive surface charge of these Nanocomposite through the carbonyl and hydroxyl functional groups on the structure of Capsaicin which have a negative charge, and following led to decreasing the surface charge of the Nanocomposite.

XRD analysis was applied to investigate the crystalline structure of $CoFe_2O_4$@ZSM-5 Nanocomposite (Figure 3). All of the significant peaks of the crystalline structure of the nanocomposite have seen and marked by a star on the XRD pattern. Slightly broad peaks (while no shift is observed) can be able to prove the small crystalline size of the Nanocomposite.

VSM analysis was applied to investigating the magnetic properties of $CoFe_2O_4$@ZSM-5 Nanocomposite. The hysteresis curves of $CoFe_2O_4$@ZSM-5 Nanocomposite are depicted in Figure 4. Saturation magnetization value of $CoFe_2O_4$@ZSM-5 Nanocomposite was found 46 emu/g. However, these saturation magnetization of modified Nanocomposite is suitable to be applied as MRI imaging agents.

3.2. Loading efficacy and *in vitro* release of capsaicin

Loading of the Capsaicin into the $CoFe_2O_4$@ZSM-5 Nanocomposite was evaluated 153 µg Capsaicin per mg of $CoFe_2O_4$@ZSM-5 Nanocomposite with the drug loading efficiency of 28%. The results represented that Capsaicin was successfully loaded into the $CoFe_2O_4$@ZSM-5 Nanocomposite. The *in vitro* release profile of Capsaicin from Capsaicin loaded synthesized $CoFe_2O_4$@ZSM-5 Nanocomposite are depicted in Figure 5. It has been shown that the release profile of the $CoFe_2O_4$@ZSM-5 Nanocomposite in acidic medium (pH = 5.5) represented a significant release (55%, at first hour) whilst in neutral medium (pH = 7.4), initial release was 11%. The total amount of Capsaicin release in acidic medium (pH = 5.5) is nearly 50% superior in

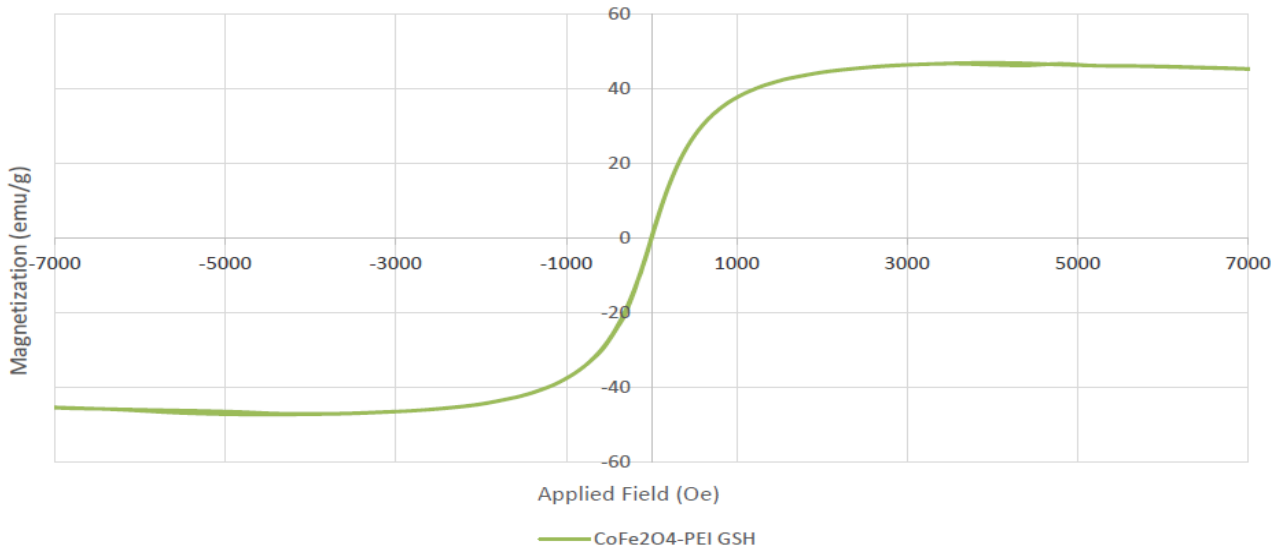

Figure 4. VSM analysis of $CoFe_2O_4$@ZSM-5 nanocomposite.

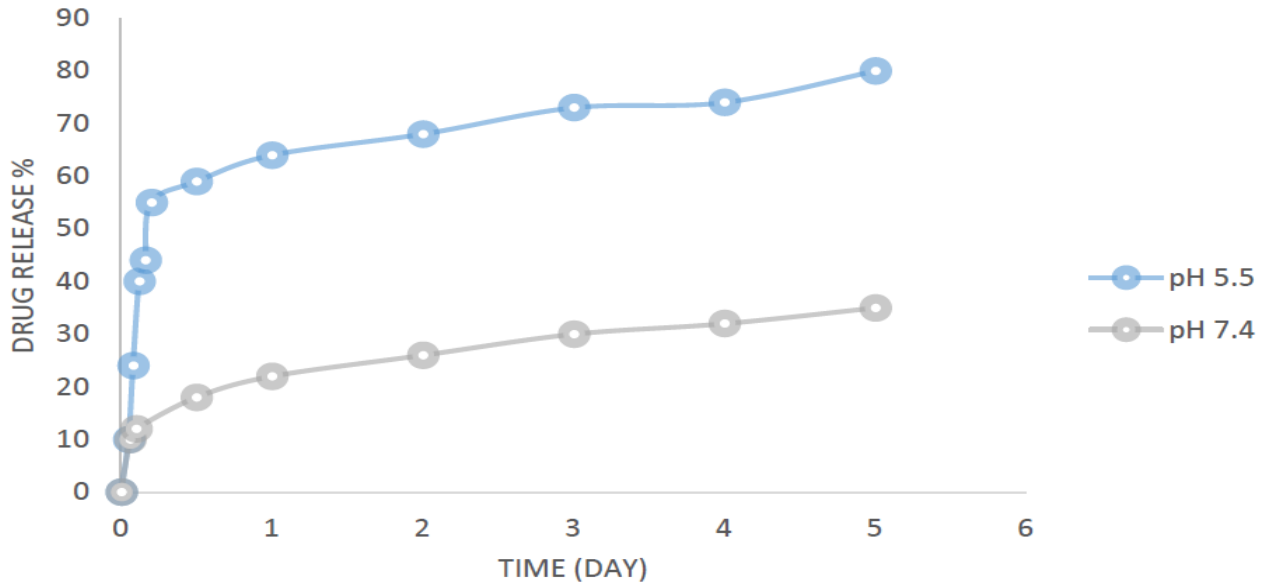

Figure 5. *in vitro* release profile of capsaicin from capsaicin $CoFe_2O_4$@ZSM-5 at different pH's.

comparison with the neutral medium (pH = 7.4). The *in vitro* drug release profile investigation successfully proved that $CoFe_2O_4$@ZSM-5 Nanocomposite is pH sensitive platform that can release the sensitizer/drug payload through the cancer cells microenvironment.

3.3. *In* vitro cytotoxicity

The $CoFe_2O_4$@ZSM-5 Nanocomposite and Capsaicin loaded $CoFe_2O_4$@ZSM-5 Nanocomposite were evaluated in terms of *in vitro* cytotoxicity which are illustrated in Figure 6. The IC_{50} of $CoFe_2O_4$@ZSM-5 Nanocomposite and free Capsaicin were specified to be 65 and 32.1 µg/mL, respectively. The concentration effect of the Capsaicin loaded $CoFe_2O_4$@ZSM-5 Nanocomposite on cell viability after incubation represented that by increasing the concentration of the Capsaicin loaded $CoFe_2O_4$@ZSM-5 Nanocomposite from 20 to 100

μg/mL, the cell viability dropped down nearly 20%, while there was no considerable toxicity for unloaded $CoFe_2O_4$@ZSM-5 Nanocomposite. Therefore, the low toxicity of the Capsaicin loaded $CoFe_2O_4$@ZSM-5 Nanocomposite to cells was proof to demonstrate the potential medicinal and biological application of the $CoFe_2O_4$@ZSM-5 Nanocomposite.

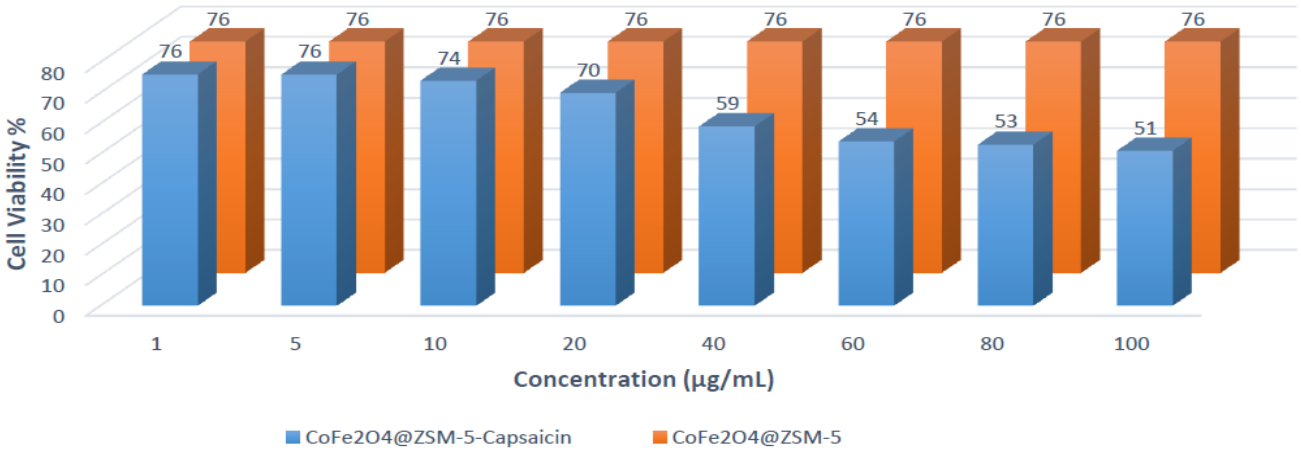

Figure 6. Cell viability of $CoFe_2O_4$@ZSM-5 and $CoFe_2O_4$@ZSM-5-capsaicin

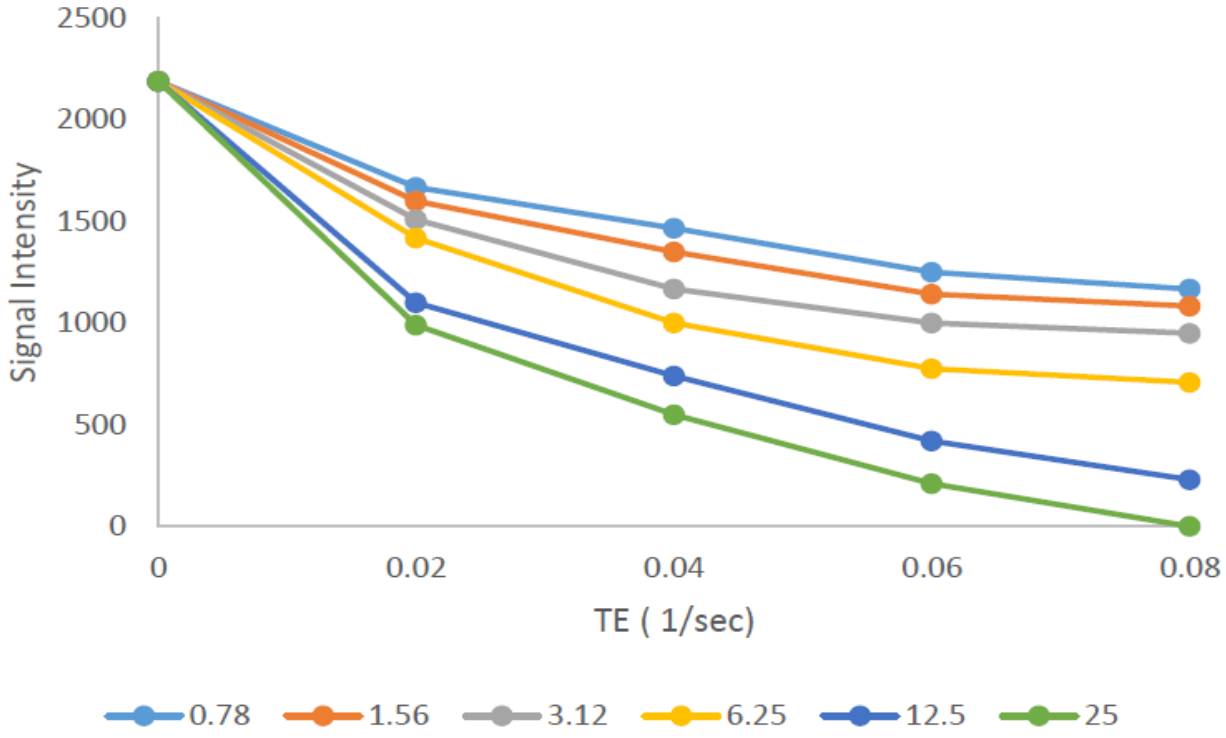

Figure 7. T_2 relaxation curves of $CoFe_2O_4$@ZSM-5-Capsaicin MNPs in different concentrations as well as in 3% phantom agar gel (0.78–40 μg/mL) scanned under a MRI scanner

3.4. *In* vitro magnetic resonance imaging

Nanocomposite has unique and considerable magnetic properties. Therefore, they can be able to apply as MRT contrast agent. This technique could improve and increase the differentiations between the target tissue [17]. In this section, *in vitro* MRI feature of Capsaicin loaded into $CoFe_2O_4$@ZSM-5 Nanocomposite was investigated. By enhancing the concentration of the nanoparticles, the T_2-weighted signals will decrease. Furthermore, by enhancing the concentration of the nanoparticles, the transverse relaxation times will decrease too. In accordance with the outputs, the linear equation in terms of increasing order of transverse relaxation rate r_2 ($1/T_2$) versus the metal concentration represented. T_2 relaxivity (r_2) was evaluated 260.36 s^{-1} μg^{-1}mL for $CoFe_2O_4$@ZSM-5-Capsaicin Nanocomposite (Figure 7, Figure 8). It should be noted that, based on the results, the prepared $CoFe_2O_4$@ZSM-5-Capsaicin Nanocomposite is an appropriate choice for MRI contrast agent application, hence, *in vivo* analysis is needed to prove this concept.

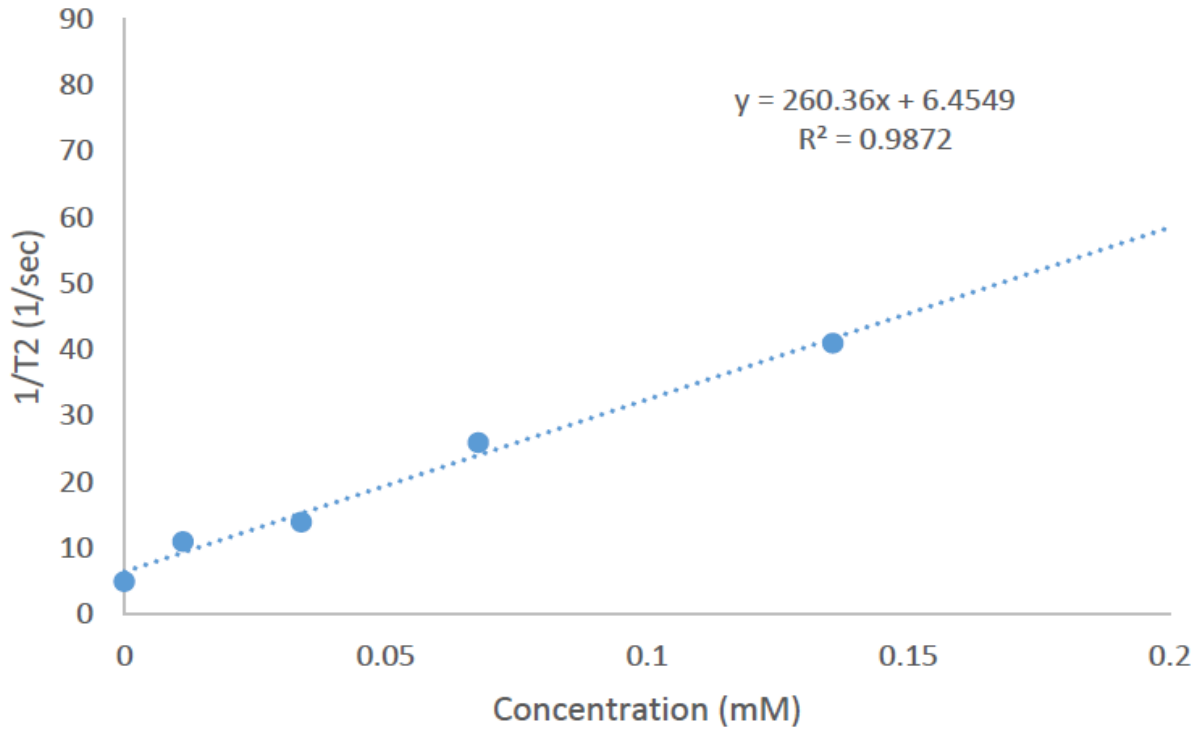

Figure 8. Plot of 1/T2 versus metal concentration of the $CoFe_2O_4$@ZSM-5 and its corresponding linear regression.

3.5. Cellular uptake investigation

Flow cytometry analysis applied to investigate the cellular uptake of Capsaicin loaded into the Nanocomposite. For this purpose, the negative control is the cells without any Capsaicin, which shown auto fluoresce. Significant Capsaicin fluorescence discovered while the SK-N-MC cells were incubated with Capsaicin loaded $CoFe_2O_4$@ZSM-5 Nanocomposite. Also, the mean fluorescence intensity of the Capsaicin for both Capsaicin and $CoFe_2O_4$@ZSM-5-Capsaicin Nanocomposite had been above the negative control cells.

4. Conclusion

To conclude, we synthesized and characterized a novel and promising specific pH-stimuli-responsive tumor-targeted DDS. Analysis of *in vitro* release profile demonstrated a pH sensitive biphasic release. This system can lead to a rebate of side-effects. The Capsaicin loaded Nanocomposite represented promising and admissible biocompatibility as well as showing higher toxicity versus SK-N-MC cells in comparison with control group.

Furthermore, uptake investigation proved that the effectively internalized DDS. With another perspective, the outputs of the *in vitro* MRI investigation demonstrated that the final Nanocomposite, has a great potential to be utilized as MRI contrast agent. Eventually, encapsulation of the Capsaicin to the multilayer Nanocomposite had considerable uptake and would be promising and effectively choice for specific pH-stimuli-responsive tumor-targeted DDS and other theranostic applications.

Conflict of Interest

The authors declare that they have no conflict of interests.

Acknowledgments

None declared.

References

[1] Ries LA, Harkins D, Krapcho M, Mariotto A, Miller B, Feuer EJ, et al. SEER cancer statistics review, 1975-2003. 2006.

[2] Torre LA, Bray F, Siegel RL, Ferlay J, Lortet-Tieulent J, Jemal A. Global cancer statistics, 2012. CA: a cancer journal for clinicians. 2015;65(2):87-108.

[3] Siegel RL, Miller KD, Jemal A. Cancer statistics, 2016. CA: a cancer journal for clinicians. 2016;66(1):7-30.

[4] Siegel RL, Miller KD, Fedewa SA, Ahnen DJ, Meester RG, Barzi A, et al. Colorectal cancer statistics, 2017. CA: a cancer journal for clinicians. 2017;67(3):177-93.

[5] Marzouni HZ, Tarkhan F, Aidun A, Shahzamani K, Tigh HRJ, Malekshahian S, et al. Cytotoxic Effects of Coated Gold Nanoparticles on PC12 Cancer Cell. Galen Medical Journal. 2018;7:1110.

[6] Farjadian F, Moghoofei M, Mirkiani S, Ghasemi A, Rabiee N, Hadifar S, et al. Bacterial components as naturally inspired nano-carriers for drug/gene delivery and immunization: Set the bugs to work? Biotechnology advances. 2018.

[7] Karimi M, Mansouri MR, Rabiee N, Hamblin MR. Drug delivery approaches. Advances in Nanomaterials for Drug Delivery: Polymeric, Nanocarbon, and Bio-inspired. 2018:1.

[8] Oren O, Smith BD. Eliminating cancer stem cells by targeting embryonic signaling pathways. Stem Cell Reviews and Reports. 2017;13(1):17-23.

[9] Reed JC. Drug insight: cancer therapy strategies based on restoration of endogenous cell death mechanisms. Nature Reviews Clinical Oncology. 2006;3(7):388.

[10] Agostinis P, Berg K, Cengel KA, Foster TH, Girotti AW, Gollnick SO, et al. Photodynamic therapy of cancer: an update. CA: a cancer journal for clinicians. 2011;61(4):250-81.

[11] Peer D, Karp JM, Hong S, Farokhzad OC, Margalit R, Langer R. Nanocarriers as an emerging platform for cancer therapy. Nature nanotechnology. 2007;2(12):751.

[12] Brannon-Peppas L, Blanchette JO. Nanoparticle and targeted systems for cancer therapy. Advanced drug delivery reviews. 2012;64:206-12.

[13] Nasseri B, Soleimani N, Rabiee N, Kalbasi A, Karimi M, Hamblin MR. Point-of-care microfluidic devices for pathogen detection. Biosensors and Bioelectronics. 2018.

[14] Vafajoo A, Rostami A, Parsa SF, Salarian R, Rabiee N, Rabiee G, et al. Early diagnosis of disease using microbead array technology: a review. Analytica chimica acta. 2018.

[15] Vafajoo A, Salarian R, Rabiee N. Biofunctionalized microbead arrays for early diagnosis of breast cancer. Biomedical Physics & Engineering Express. 2018;4(6):065028.

[16] Chitkara D, Mittal A, Mahato RI. Molecular Medicines for Cancer: Concepts and Applications of Nanotechnology. 2018.

[17] Na HB, Song IC, Hyeon T. Inorganic nanoparticles for MRI contrast agents. Advanced materials. 2009;21(21):2133-48.

[18] Ghasemi A, Rabiee N, Ahmadi S, Lolasi F, Borzogomid M, Kalbasi A, et al. Optical Assays Based on Colloidal Inorganic Nanoparticles. Analyst. 2018.

[19] Ghasemi A, Rabiee N, Ahmadi S, Hashemzadeh S, Lolasi F, Bozorgomid M, et al. Optical assays based on colloidal inorganic nanoparticles. Analyst. 2018;143(14):3249-83.

[20] Karimi M, Mansouri MR, Rabiee N, Hamblin MR. Polymeric and hyper-branched nanoparticles and dendrimers. Advances in Nanomaterials for Drug Delivery: Polymeric, Nanocarbon, and Bio-inspired. 2018:3.

[21] Karimi M, Mansouri MR, Rabiee N, Hamblin MR. Aptamers and pathogen-based carriers. Advances in Nanomaterials for Drug Delivery: Polymeric, Nanocarbon, and Bio-inspired. 2018.

[22] Karimi M, Mansouri MR, Rabiee N, Hamblin MR. Carbon-based nanomaterials. Advances in Nanomaterials for Drug Delivery: Polymeric, Nanocarbon, and Bio-inspired. 2018.

[23] Lu AH, Salabas EeL, Schüth F. Magnetic nanoparticles: synthesis, protection, functionalization, and application. Angewandte Chemie International Edition. 2007;46(8):1222-44.

[24] Pankhurst QA, Connolly J, Jones S, Dobson J. Applications of magnetic nanoparticles in biomedicine. Journal of physics D: Applied physics. 2003;36(13):R167.

[25] Amiri S, Shokrollahi H. The role of cobalt ferrite magnetic nanoparticles in medical science. Materials Science and Engineering: C. 2013;33(1):1-8.

[26] Karimi M, Mansouri MR, Rabiee N, Hamblin MR. Advances in Nanomaterials for Drug Delivery: Polymeric, Nanocarbon, and Bio-inspired: Morgan & Claypool Publishers; 2018.

[27] Deljoo S, Rabiee N, Rabiee M. Curcumin-hybrid Nanoparticles in Drug Delivery System. Asian Journal of Nanosciences and Materials. 2019;2(1, pp. 1-119.):66-91.

[28] Vafajoo A, Rostami A, Parsa SF, Salarian R, Rabiee N, Rabiee G, et al. Multiplexed microarrays based on optically encoded microbeads. Biomedical microdevices. 2018;20(3):66.

[29] Clark R, Lee S-H. Anticancer properties of capsaicin against human cancer. Anticancer research. 2016;36(3):837-43.

[30] Clark R, Lee J, Lee S-H. Synergistic anticancer activity of capsaicin and 3, 3′-Diindolylmethane in human colorectal cancer. Journal of agricultural and food chemistry. 2015;63(17):4297-304.

[31] Bley K, Boorman G, Mohammad B, McKenzie D, Babbar S. A comprehensive review of the carcinogenic and anticarcinogenic potential of capsaicin. Toxicologic pathology. 2012;40(6):847-73.

[32] Park K-K, Surh Y-J. Effects of capsaicin on chemically-induced two-stage mouse skin carcinogenesis. Cancer letters. 1997;114(1-2):183-4.

[33] Karimi M, Mansouri MR, Rabiee N, Hamblin MR. Advances in nature-inspired nanomaterials. Advances in Nanomaterials for Drug Delivery: Polymeric, Nanocarbon, and Bio-inspired. 2018.